Eur. Phys. J. B **43**, 297–303 (2005)
DOI: 10.1140/epjb/e2005-00057-y

THE EUROPEAN PHYSICAL JOURNAL B

The effect of iron doping in $La_{0.8}Sr_{0.2}Fe_{0.05}Co_{0.95}O_{3-\delta}$ perovskite

Z. Németh[1,a], Z. Klencsár[2], E. Kuzmann[2], Z. Homonnay[1], A. Vértes[1,2], J.M. Grenèche[3], B. Lackner[4], K. Kellner[4], G. Gritzner[4], J. Hakl[5], K. Vad[5], S. Mészáros[5], and L. Kerekes[5]

[1] Department of Nuclear Chemistry, Eötvös Loránd University, Pázmány P. s. 1/a, Budapest 1117, Hungary
[2] Research Group for Nuclear Methods in Structural Chemistry, Hungarian Academy of Sciences, Hungary
[3] Laboratoire de Physique de l'État Condensé, UMR CNRS 6087, Université du Maine, 72085 Le Mans Cedex 9, France
[4] Institute for Chemical Technology of Inorganic Materials, Johannes Kepler University, Altenbergerstrasse 69, 4040 Linz, Austria
[5] Institute of Nuclear Research of the Hungarian Academy of Sciences, 4001 Debrecen, POB 51, Hungary

Received 9 September 2004 / Received in final form 5 November 2004
Published online 15 March 2005 –

Abstract. $La_{0.8}Sr_{0.2}\,^{57}Fe_{0.05}Co_{0.95}O_{3-\delta}$ perovskite is investigated by ^{57}Fe transmission and emission Mössbauer spectroscopy, X-ray diffraction, AC magnetic susceptibility and magnetotransport measurements. Temperature dependence of the ^{57}Fe Mössbauer isomer shift, quadrupole splitting, magnetic hyperfine field, line broadening, and relative spectral area is presented in a detailed manner for $La_{0.8}Sr_{0.2}\,^{57}Fe_{0.05}Co_{0.95}O_{3-\delta}$. The oxidation state of iron is determined to be Fe^{3+}, and the presence of preferential electronic charge compensation $Fe^{3+} \rightarrow Fe^{4+}$ over that of $Co^{3+} \rightarrow Co^{4+}$ is excluded. Relaxation of iron magnetic moments reflected by the ^{57}Fe Mössbauer spectra of $La_{0.8}Sr_{0.2}\,^{57}Fe_{0.05}Co_{0.95}O_{3-\delta}$ are interpreted as evidence for the existence of superparamagnetic like Co clusters and a corresponding cluster glass magnetic phase formed below $T \approx 65$ K.

PACS. 75.47.Gk Colossal magnetoresistance – 75.50.Lk Spin glasses and other random magnets – 76.80.+y Mössbauer effect; other gamma-ray spectroscopy

1 Introduction

Following the discovery of the effect of colossal negative magnetoresistance (CMR) in doped manganite perovskites [1], a search for materials showing similar anomalous effects was started. Various transition metal compounds with different composition and crystal structure, such as Sr_2FeMoO_6 [2], $FeCr_2S_4$ [3], and $La_{0.8}Sr_{0.2}Fe_xCo_{1-x}O_3$ [4] were also found to show large magnetoresistance effect. Models aiming to shed light on the CMR effect found in manganite perovskites, and to explain the unusually strong correlation between the magnetic state of the material and its electric transport properties, are based on the theory of double exchange [5]. However, it was argued, that the assumption of a strong electron-lattice interaction is also necessary to explain the semiconducting nature of the paramagnetic phase [6,7]. This strong electron-lattice coupling is thought to be due to Jahn-Teller type distortions [7].

In contrast to manganites, in $La_{1-y}Sr_yCoO_{3-\delta}$ magnetoresistance (MR) was found not only in the neighborhood of the Curie point, but also at lower temperatures [8–11]. The origin of this negative magnetoresistance in the cobaltate perovskites is not satisfactorily understood yet. Although Jahn-Teller type distortions may also occur in $La_{1-y}Sr_yCoO_{3-\delta}$, the conduction mechanism in these materials cannot be explained on the basis of the conventional double exchange model [9]. At the same time, the spin state of the cobalt ions is thought to play a decisive role in the electronic transport and magnetic properties of the cobaltate perovskites [9]. The substitution of divalent strontium in the rare-earth site can convert trivalent cobalt ions into tetravalent state. Apart from the formation of tetravalent cobalt ions, doping of La by Sr may result in an increased number of oxygen vacancies as well. The competition between the two effects was demonstrated by Mineshige et al. [12]. Strontium substitution also alters the electronic transport, the magnetic, as well as the MR properties of these materials [8,11].

Barman et al. found that a small exchange of cobalt by iron greatly enhances negative magnetoresistance in $La_{0.8}Sr_{0.2}Fe_xCo_{1-x}O_3$ [4]. At low temperatures, magnetoresistance in $La_{0.8}Sr_{0.2}Fe_xCo_{1-x}O_3$ shows a similar tendency as observed in $La_{1-x}Sr_xCoO_3$. Below 50 K the magnetoresistance increases rapidly with decreasing temperature, but the extent of the MR in the iron doped compound exceeds the one in the iron free material. Between 50 K and 150 K the magnetoresistance is close to zero, but from about 150 K it increases up to ∼300 K where it seems to saturate. However, the high temperature magnetoresistance was not

[a] e-mail: hentes@ludens.elte.hu

confirmed by other authors [13,14]. Iron substitution was also found to lead to an increase of the unit cell volume in $La_{0.8}Sr_{0.2}Fe_xCo_{1-x}O_3$ [15,16], which was interpreted as an increase in the number of oxygen vacancies in the iron substituted compounds.

In order to gain further insight into the effect of iron in enhancing the negative magnetoresistance in $La_{0.8}Sr_{0.2}Fe_xCo_{1-x}O_3$ perovskites with low iron concentration, $La_{0.8}Sr_{0.2}{}^{57}Fe_{0.05}Co_{0.95}O_{3-\delta}$ was prepared and investigated by ^{57}Fe transmission Mössbauer spectroscopy (TMS), ^{57}Fe emission Mössbauer spectroscopy (EMS), X-ray diffraction (XRD), AC magnetic susceptibility and magnetotransport measurements.

2 Experimental

$La_{0.8}Sr_{0.2}{}^{57}Fe_{0.05}Co_{0.95}O_{3-\delta}$ was prepared in the following way. First, $La_{0.8}Sr_{0.2}CoO_3$ samples were fabricated via the citric acid-ethylene glycol method. The stoichiometric amounts of $La(NO_3)_3{\cdot}6H_2O$, $SrCO_3$ and $Co(NO_3)_2{\cdot}6H_2O$ were dissolved in 50 ml of concentrated nitric acid. ^{57}Fe metal was dissolved in nitric acid and the respective amount was added to the nitric acid solution. The solution was diluted with 200 ml water. 30 g citric acid and 8 g ethylene glycol were then added. The aqueous solution was evaporated until a brown gel was obtained. The gels were dried under vacuum at 125 °C. The residues were ground, first heated to 500 °C, kept at this temperature for two hours and then heated to 800 °C. The heating rates were 5 K min^{-1}. The samples were kept at 800 °C for five hours. Upon ballistic cooling the samples were ground and compacted at 750 MPa into discs of 10 mm diameter. The specimens were then sintered in air at 1200 °C for 24 hours. Heating rates were 3 K min^{-1}, cooling rates 10 K min^{-1}. The oxygen content was analyzed by iodometric titration.

^{57}Fe TMS measurements were carried out on a powdered sample in transmission geometry in a temperature controlled flow-through type liquid nitrogen cryostat (Leybold) and in a temperature controlled helium bath cryostat. The low temperature measurements were carried out as a function of temperature in the range of 4.2 K to 300 K. During the measurements the temperature of the $La_{0.8}Sr_{0.2}{}^{57}Fe_{0.05}Co_{0.95}O_{3-\delta}$ sample was kept constant with a precision of $\Delta T \approx \pm 0.5$ K. The γ rays were provided by a ^{57}Co(Rh) source with 10^9 Bq activity. In the case of the spectra taken at 30 K and 40 K the ^{57}Co(Rh) source was cooled at the same temperature, otherwise the source was maintained at room temperature.

The emission Mössbauer measurements on the $La_{0.8}Sr_{0.2}{}^{57}Fe_{0.05}Co_{0.95}O_{3-\delta}$ sample were carried out using ^{57}Co doping with the following technique. The aqueous solution of $^{57}Co(NO_3)_2$, containing 0.1 M nitric acid, with an activity of 100 MBq was let evaporate to complete dryness under an infrared lamp. Then the dry residue was re-dissolved and transferred drop by drop to a pellet of the $La_{0.8}Sr_{0.2}{}^{57}Fe_{0.05}Co_{0.95}O_{3-\delta}$ sample using 200 μl absolute ethanol. After evaporation of the ethanol, the dry sample was heated for 2 hours at 1000 °C (diffusion thermal treatment) and then cooled down to room temperature in O_2 atmosphere. XRD measurement confirmed that the perovskite structure and the composition of the original sample were not changed during the heat treatment. Mössbauer spectra were recorded at 4.2 K in a helium bath cryostat and at room temperature using the conventional emission geometry.

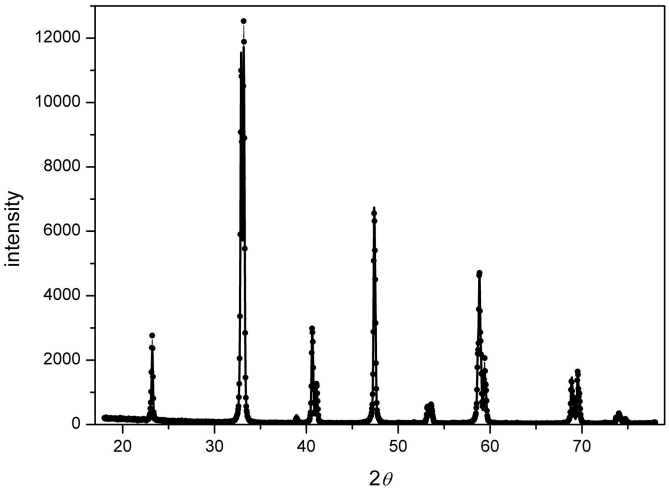

Fig. 1. X-ray diffractogram of $La_{0.8}Sr_{0.2}{}^{57}Fe_{0.05}Co_{0.95}O_3$.

^{57}Fe isomer shift values of TMS and EMS spectra are given relative to α-iron at room temperature. Mössbauer spectra were analyzed with version 3.0 of the MossWinn program [17].

Temperature dependence of AC magnetic susceptibility of $La_{0.8}Sr_{0.2}{}^{57}Fe_{0.05}Co_{0.95}O_{3-\delta}$ was measured at frequencies of 133 Hz, 1 kHz and 10 kHz using AC magnetic field of 365 A/m in the temperature range of 7–225 K, while magnetotransport measurement was performed by standard four point contact method.

3 Results

The powder X-ray diffraction pattern of $La_{0.8}Sr_{0.2}{}^{57}Fe_{0.05}Co_{0.95}O_{3-\delta}$ is shown in Figure 1. The diffraction lines are characteristic for the perovskite structure of doped cobaltates (for comparison, see e.g. Refs. [4,11]).

Figure 2 shows AC magnetic susceptibility, resistivity and magnetoresistance of $La_{0.8}Sr_{0.2}{}^{57}Fe_{0.05}Co_{0.95}O_{3-\delta}$, as a function of temperature. The real component of χ_{AC} (χ') is of broad peak character. χ' starts to rise exponentially at 180 K with decreasing temperature, peaks up at 80 K and shows some additional substructure at 60–65 K. The height at 80 K is frequency dependent, which is a direct indication of slow spin dynamics. Both the frequency dependence of the maximum of χ' and the long high temperature tail indicate the spin glass (SG) region of the magnetic phase diagram. $\chi'_{133\,\mathrm{Hz}}/\chi'_{1000\,\mathrm{Hz}}$ susceptibility ratio indicates changes in spin dynamics at 65 K and 101 K. Above 101 K the susceptibility is frequency independent. Applying the Curie-Weiss formula for the high temperature part ($T > 185$ K) of the AC susceptibility 120 K can be identified as Curie temperature T_c with 3.2 μ_B/f.u. effective magnetic moment. Abrupt change in

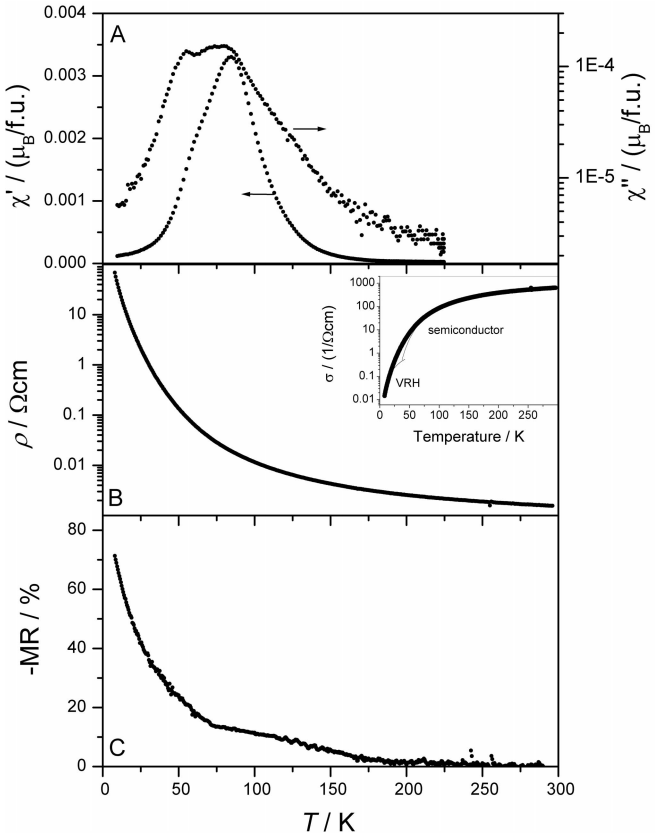

Fig. 2. The temperature dependence of A: real and imaginary components of AC magnetic susceptibility ($f = 133$ Hz), B: resistivity (insert: conductivity with semiconductor and VRH model fittings), and C: magnetoresistance measured on $La_{0.8}Sr_{0.2}\,^{57}Fe_{0.05}Co_{0.95}O_{3-\delta}$.

the slope of the linear trend of $1/\chi'_{133\text{ Hz}}$ can be observed at 182 K. This part of the curve indicates the presence of a weak ferromagnetic ordering in the sample. At 170 K linearity is lost and the magnetic energy dissipation over a single cycle starts to increase sharply at 150 K, which can be seen in the imaginary component (χ'') of the AC susceptibility. It is worth noting, that around T_c a weak substructure can be identified in the χ''.

The temperature dependence of resistivity corresponds to semiconductor like variation, diverging at $T \to 0$ K, which is typical for cobaltates in the spin glass phase (Fig. 2). While at $T > 50$ K resistivity variation can be fitted with a semiconductor model $\rho \approx \exp(E/kT)$, $E = 23.2$ meV, at low temperature end ($T < 20$ K) the resistivity curve can be fitted with a variable range hopping model, $\rho \approx \exp(T_0/T)^{1/2}$ with $T_0 = 329$ K.

The MR ratio measured in 7.5 T external magnetic field increases with decreasing temperature from room temperature (Fig. 2). It achieves values up to –70% at lowest temperatures, although there are significant kinks in the curve at 65 K and around 180 K. The traces of a 'peak' between the two kinks resembles to peaks in magnetoresistivity observed around T_c in perovskites.

Figure 3 shows the ^{57}Fe transmission Mössbauer spectra of $La_{0.8}Sr_{0.2}\,^{57}Fe_{0.05}Co_{0.95}O_{3-\delta}$ at selected temperatures. The spectra observed between 120 K and room temperature show a broad absorption peak that can be best fitted with a doublet showing a small (∼0.2 mm s^{-1}) quadrupole splitting. The corresponding ^{57}Fe Mössbauer parameters are presented in Table 1. Below about 120 K a magnetic sextet develops gradually, referring to iron cations undergoing magnetic relaxation that slows down (below the Larmor precession rate of the ^{57}Fe nucleus) with decreasing temperature.

Table 1. ^{57}Fe transmission Mössbauer parameters of $La_{0.8}Sr_{0.2}\,^{57}Fe_{0.05}Co_{0.95}O_{3-\delta}$ at selected temperatures (in round brackets the error of the last digit obtained by the fitting procedure is shown).

T / K	δ / mm s^{-1}	Δ / mm s^{-1}	$\langle B\rangle$ / T	Γ / mm s^{-1}
4.2	0.391(1)	0	40.0	0.30(1)
40	0.401(6)	0	33.2	0.32(1)
57	0.41(1)	0	26.0	0.36(1)
67	0.41(1)	0	20.2	0.73(2)
125	0.390(1)	0.222(3)	0	0.402(4)
155	0.380(1)	0.209(1)	0	0.377(1)
200	0.349(1)	0.198(2)	0	0.355(3)
300	0.290(1)	0.185(2)	0	0.356(3)

Table 2. ^{57}Fe EMS parameters of $La_{0.8}Sr_{0.2}\,^{57}Fe_{0.05}\times Co_{0.95}O_{3-\delta}$ at temperatures 300 K and 4.2 K.

T / K	δ / mm s^{-1}	Δ / mm s^{-1}	$\langle B\rangle$ / T	Γ / mm s^{-1}
4.2	0.45(1)	0	46.2	0.33(3)
300	0.321(3)	0.21(1)	0	0.46(1)

The emission Mössbauer spectra and the corresponding Mössbauer parameters of the ^{57}Co doped $La_{0.8}Sr_{0.2}\,^{57}Fe_{0.05}Co_{0.95}O_{3-\delta}$ sample are presented in Figure 4 and Table 2, respectively. At room temperature only a single line appears whose ^{57}Fe Mössbauer parameters are close to those obtained from the room temperature transmission Mössbauer spectrum of this perovskite. At 4.2 K one can see a sextet with a characteristic magnetic field of 46.2 T, but with broad Mössbauer lines.

4 Discussion

For evaluating the ^{57}Fe transmission Mössbauer spectra of $La_{0.8}Sr_{0.2}\,^{57}Fe_{0.05}Co_{0.95}O_{3-\delta}$ between 120 K and 300 K a quadrupole doublet was used as a fitting model. In this temperature interval an anomalous peak in the temperature dependence of the Mössbauer line width (Γ) is observable at $T \approx 150$ K, which refers to a phase transition at this temperature (Fig. 5). The observation that the losses in AC magnetic susceptibility (Fig. 2) start to rise exponentially at around the same temperature interval suggests that this phase transition is of magnetic origin. The same phase transition is visualized in the temperature dependence of the ^{57}Fe quadrupole splitting (Δ, Fig. 6) and isomer shift (δ, Fig. 7), and (somewhat less obviously) in the temperature dependence of the normalized spectrum area (Fig. 8) as well.

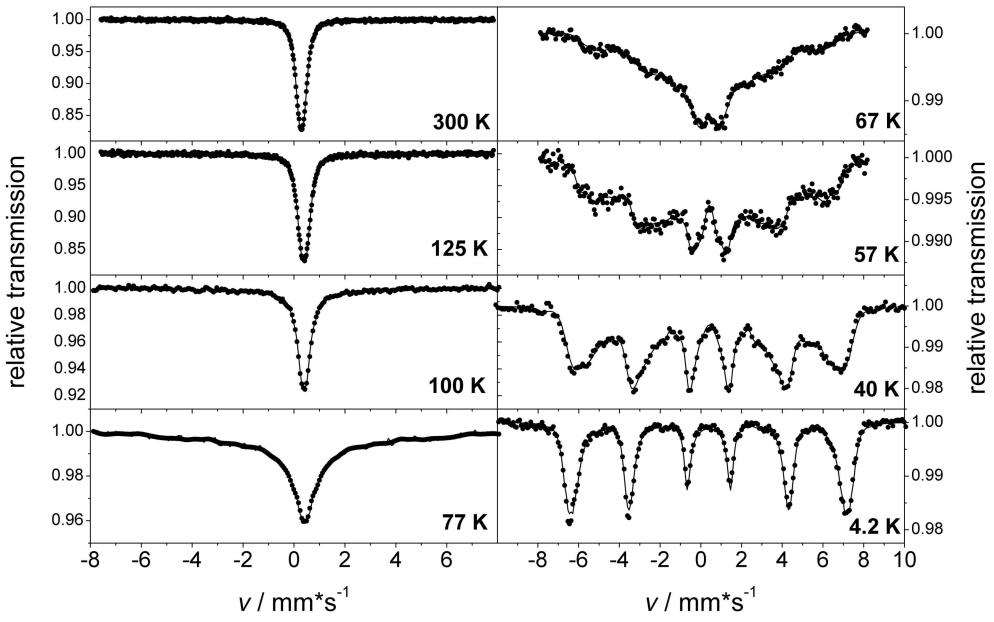

Fig. 3. ^{57}Fe Mössbauer spectra of $La_{0.8}Sr_{0.2}\,{}^{57}Fe_{0.05}Co_{0.95}O_{3-\delta}$ at selected temperatures.

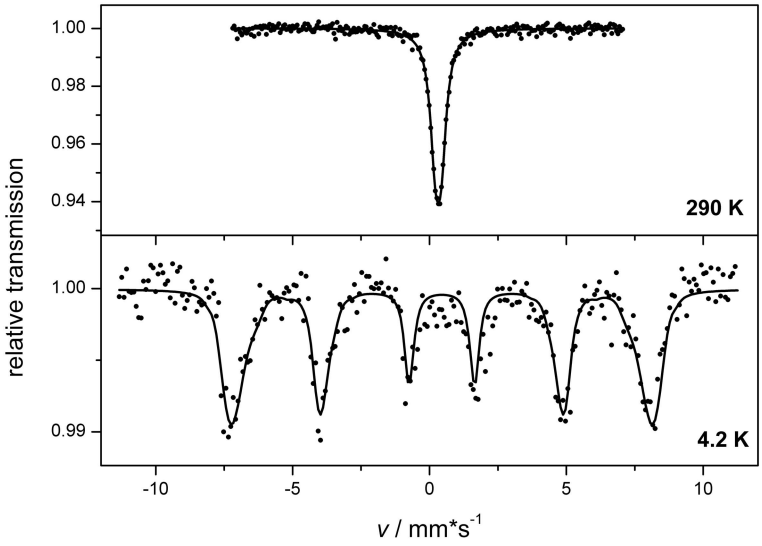

Fig. 4. ^{57}Fe emission Mössbauer spectra of $La_{0.8}Sr_{0.2}\,{}^{57}Fe_{0.05}Co_{0.95}O_{3-\delta}$ at 290 K (top) and at 4.2 K (bottom).

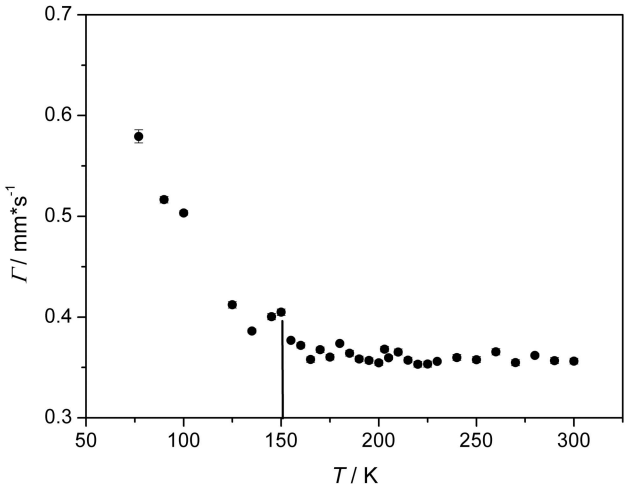

Fig. 5. Temperature dependence of the line width of the fitted Mössbauer doublet of $La_{0.8}Sr_{0.2}\,{}^{57}Fe_{0.05}Co_{0.95}O_{3-\delta}$.

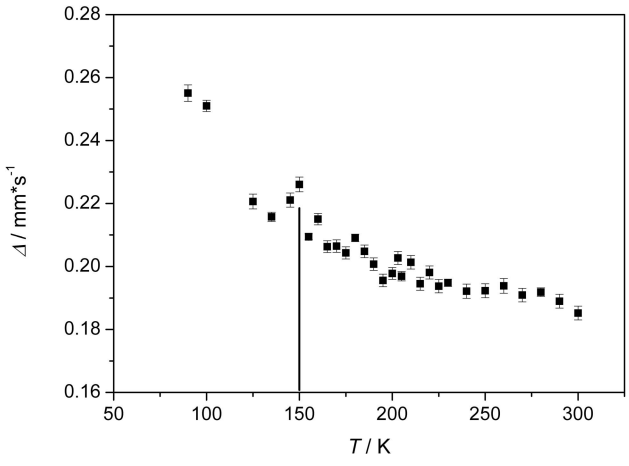

Fig. 6. Temperature dependence of the quadrupole splitting of the paramagnetic component of the Mössbauer spectra of $La_{0.8}Sr_{0.2}\,{}^{57}Fe_{0.05}Co_{0.95}O_{3-\delta}$.

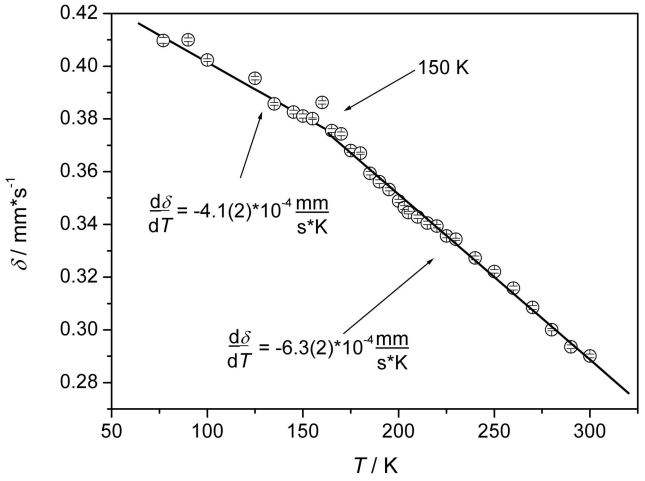

Fig. 7. The ^{57}Fe isomer shift of the doublet of $La_{0.8}Sr_{0.2}\,^{57}Fe_{0.05}Co_{0.95}O_{3-\delta}$ as a function of temperature.

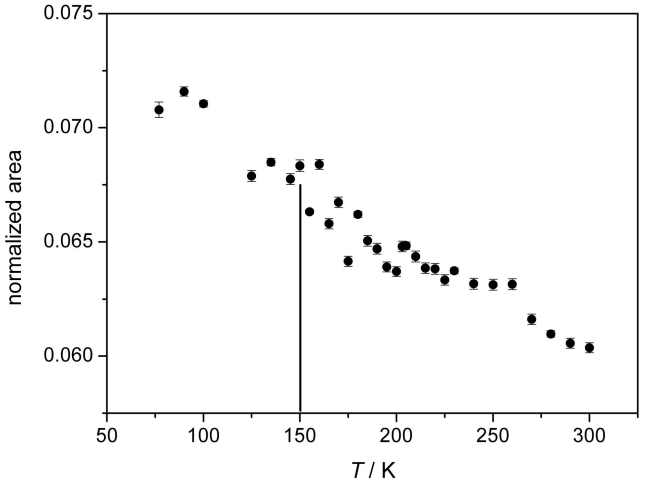

Fig. 8. The normalized area of the ^{57}Fe Mössbauer doublet of $La_{0.8}Sr_{0.2}\,^{57}Fe_{0.05}Co_{0.95}O_{3-\delta}$.

The change in the slope of the ^{57}Fe isomer shift (Fig. 7) at around $T \approx 150$ K refers to a change in the vibrational state of iron, which in the frame of the Debye-model can be expressed as a change in the so called effective vibrational mass ($M_{\rm vibr}$) [18]:

$$M_{\rm vibr} = -\frac{3 \cdot k_B}{\frac{d\delta}{dT} \cdot c}$$

where k_B is the Boltzmann constant and c is the speed of light in vacuum. In the present case we observe that

$$\frac{M_{\rm vibr}(T < 150\ {\rm K})}{M_{\rm vibr}(T > 150\ {\rm K})} \approx \frac{3}{2}$$

which means that below $T \approx 150$ K iron is more tightly bound to its neighbors than above this temperature. The additional force acting on iron below 150 K is likely to be of magnetic origin.

The normalized area of the Mössbauer spectrum (A_N, the area under the Mössbauer spectrum divided by the base line) is proportional to the Mössbauer-Lamb factor (f) that is a function of the $\langle x^2 \rangle$ mean square displacement of the vibrating iron atoms: $f = \exp(-k^2\langle x^2 \rangle)$, where k denotes the wave number of the Mössbauer photon. In the frame of the Debye model, f, and consequently A_N, should decrease with temperature monotonically. The dependence of A_N on temperature (Fig. 8) is therefore anomalous below about 150 K where A_N seems to be constant or slightly increasing with temperature. This anomalous temperature dependence ends by a sharp drop in A_N simultaneously with the set-in of the phase transition when the temperature is raised above $T \approx 150$ K (Fig. 8). This drop in A_N can be interpreted as a sudden increase in $\langle x^2 \rangle$ of iron while $La_{0.8}Sr_{0.2}\,^{57}Fe_{0.05}Co_{0.95}O_{3-\delta}$ undergoes a magnetic phase transition (Fig. 2). The origin of this effect may be the same as that of the anomalous lattice expansion found in $La_{1-x}Sr_xCoO_{3-\delta}$ above T_C [19,20], i.e. electron localization on transition metal cations and the connected cooperative displacement of the O^{2-} ions, which results in an increase of the mean transition metal - oxygen bond length.

These observations show that in $La_{0.8}Sr_{0.2}\,^{57}Fe_{0.05}Co_{0.95}O_{3-\delta}$ there is a magnetic exchange interaction between iron and cobalt, as a consequence of which the ^{57}Fe Mössbauer parameters reflect the magnetic transition of the cobalt subsystem at around $T \approx 150$ K. However, this magnetic transition does not result in a preferred orientation of iron magnetic moments, and therefore the magnetic six line pattern does not appear in the ^{57}Fe Mössbauer spectrum of $La_{0.8}Sr_{0.2}\,^{57}Fe_{0.05}Co_{0.95}O_{3-\delta}$ at this temperature (Fig. 3). Instead, below $T \approx 150$ K the relaxation rate of the magnetic moment of iron cations decreases with decreasing temperature, which is visualized as an increase in the Mössbauer line width (Fig. 5) that turns into an evolution of the magnetic field distribution under $T_c \approx 120$ K (Figs. 3 and 10). The observation that the slowing down of relaxation of iron spins begins simultaneously with the magnetic ordering of the Co subsystem suggests that the Fe-Co magnetic exchange interaction is stronger than the Co-Co magnetic exchange interaction leading to magnetic ordering at $T \approx 150$ K.

In the temperature range of 4.2 K $\leq T \leq$ 120 K the TMS spectra of $La_{0.8}Sr_{0.2}\,^{57}Fe_{0.05}Co_{0.95}O_{3-\delta}$ was fitted with a combination of a paramagnetic doublet and a distribution of magnetic sextets. The ratio of the paramagnetic component starts to fall with decreasing temperature at around $T_c \approx 120$ K, and it disappears below about 65–70 K (Fig. 9) that coincides with the temperature where – according to the AC susceptibility measurement – the spin dynamics changes. Moreover, the ratio of the doublet and the sextets turns at about 100 K, which temperature was found to be the boundary between the frequency dependent and frequency independent parts of χ'.

The distributions of the hyperfine field, reflected by the Mössbauer spectra recorded between 4.2 K and 100 K, are plotted in Figure 10. As it can be seen, a small distribution

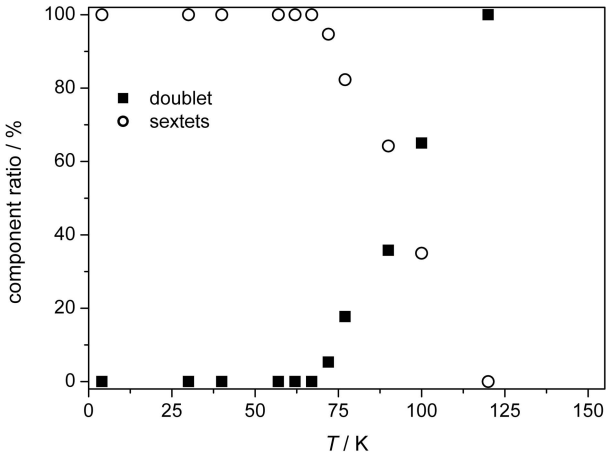

Fig. 9. Ratio of paramagnetic and magnetic subspectra in the TMS spectra of $La_{0.8}Sr_{0.2}\,^{57}Fe_{0.05}Co_{0.95}O_{3-\delta}$ between 4.2 K and 150 K.

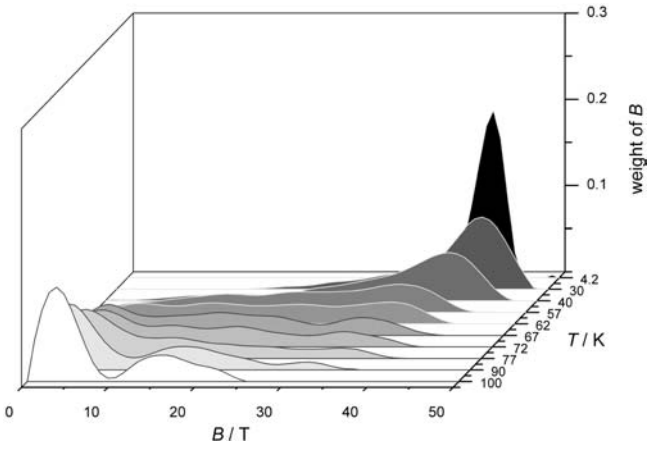

Fig. 10. Magnetic field distribution of the magnetic component in the ^{57}Fe Mössbauer spectra of $La_{0.8}Sr_{0.2}\,^{57}Fe_{0.05}Co_{0.95}O_{3-\delta}$ between 4.2 K and 100 K.

of hyperfine fields remains even at 4.2 K. This indicates that besides the relaxation phenomenon, broadening of the ^{57}Fe Mössbauer peaks is also contributed to by a static distribution of hyperfine magnetic fields originated from Co presence in the next neighborhood of ^{57}Fe nuclei.

The fact that the iron magnetic moments reflect a tendency for the freezing of the relaxation of iron spins with decreasing temperature indicates the formation of spin- or cluster glass phases, which is in accordance with the results of the AC magnetic susceptibility measurements of $La_{0.8}Sr_{0.2}\,^{57}Fe_{0.05}Co_{0.95}O_{3-\delta}$ (Fig. 2) displaying substantial blocking below $T \approx 65$ K.

By doping $La_{0.8}Sr_{0.2}\,^{57}Fe_{0.05}Co_{0.95}O_{3-\delta}$ with a minute amount of ^{57}Co, one can study the hyperfine interactions of ^{57}Fe in a lattice site where Co tends to be bounded chemically. Namely, while during the doping procedure radioactive ^{57}Co is introduced into the system, the Mössbauer experiment is carried out by the help of the 14.4 keV gamma ray emitted by the ^{57}Fe nucleus formed via the electron capture decay of ^{57}Co. Considering the relatively low level of iron ($x = 0.05$) present in this system,

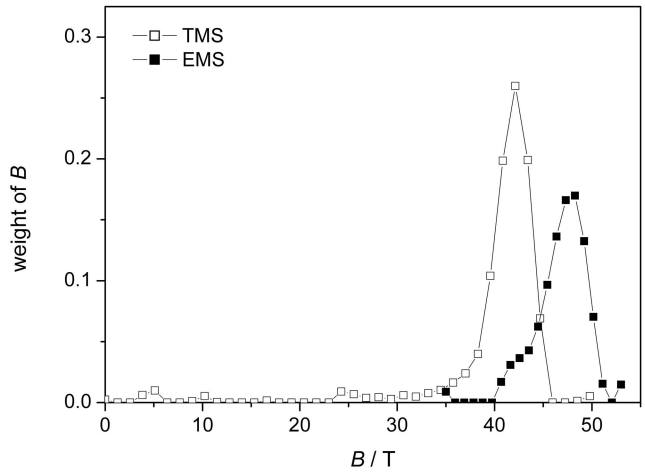

Fig. 11. Magnetic distribution of the transmission Mössbauer spectrum (TMS) and the emission Mössbauer spectrum (EMS) of $La_{0.8}Sr_{0.2}\,^{57}Fe_{0.05}Co_{0.95}O_{3-\delta}$ taken at 4.2 K.

these parameters can be taken as representative for iron cations with Co as nearest transition metal neighbors. The room temperature ^{57}Fe Mössbauer parameters obtained for these iron cations are very close to those obtained from the ^{57}Fe transmission Mössbauer spectrum of the 5% (relative to Co) iron originally built into the system (Tab. 2). This suggests that in $La_{0.8}Sr_{0.2}\,^{57}Fe_{0.05}Co_{0.95}O_{3-\delta}$ majority of iron has cobalt as nearest neighbor transition metal cation, i.e. the occurrence of cobalt-free iron clusters must be rare. Furthermore, it indicates that iron and cobalt are in a similar oxygen ligand environment in this compound. At $T = 4.2$ K the EMS spectrum of $La_{0.8}Sr_{0.2}\,^{57}Fe_{0.05}Co_{0.95}O_{3-\delta}$ (Fig. 4) displays an average hyperfine magnetic field ($\langle B \rangle$) of 46.2 T (Tab. 2), which is significantly smaller than that expected for high spin Fe^{3+} (∼50 to 55 T). At the same time, the magnetic sextet displays broad Mössbauer lines, and a corresponding distribution of the magnetic field. Although a very similar magnetic distribution can be found in the ^{57}Fe TMS spectrum of $La_{0.8}Sr_{0.2}\,^{57}Fe_{0.05}Co_{0.95}O_{3-\delta}$ at $T = 4.2$ K, the average magnetic field of the EMS spectrum is higher than that of the TMS spectrum (Tab. 1). The difference of the magnetic distributions of the TMS and EMS spectra can be seen in Figure 11. While in the case of the transmission spectrum the magnetic distribution function shows a characteristic peak at about 42 T with a small shoulder towards lower magnetic fields, in the case of the emission Mössbauer spectrum a broader peak shows up at around 48 T. This difference in the magnetic distributions can be understood if one takes into account that the EMS measurement corresponds to iron cations in cobalt sites, and so it reflects not only the local magnetic environment of the iron containing cobalt clusters, but also those of the iron free regions. The fact that the (originally) iron free clusters can be characterized by higher hyperfine magnetic fields, may also be a consequence of their magnetic relaxation being slower because of their larger size. This suggests that due to iron substitution relatively large cobalt clusters become broken up into smaller ones.

In $La_{0.8}Sr_{0.2}\,^{57}Fe_{0.05}Co_{0.95}O_{3-\delta}$ only small magnetoresistance effect can be observed at room temperature. The MR ratio increases monotonically with decreasing temperature, however the dMR/dT changes abruptly at 65 K and 180 K. These two transition temperatures are well identified in AC magnetic susceptibility records.

The temperature dependence of the relaxation rate of iron spins (as most obviously reflected by Figs. 3 and 10) clearly correlates with that of magnetoresistance (Fig. 2). This suggests that negative magnetoresistance in $La_{0.8}Sr_{0.2}\,^{57}Fe_{0.05}Co_{0.95}O_{3-\delta}$ may be related to the rate of superparamagnetic-like relaxation of nanometer sized magnetic clusters. The slowing down of magnetic relaxation, at the same time, may be a consequence of an increasing cluster size or the gradual freezing of the glassy spin structure with decreasing temperature.

Our results indicate that $La_{0.8}Sr_{0.2}\,^{57}Fe_{0.05}Co_{0.95}O_{3-\delta}$ develops a cluster glass magnetic structure below $T \approx 65$ K (Fig. 2). We suggest that the magnetic behavior of iron reflected by the ^{57}Fe Mössbauer spectra of $La_{0.8}Sr_{0.2}\,^{57}Fe_{0.05}Co_{0.95}O_{3-\delta}$ (Fig. 10) is also a consequence of the relaxation of small superparamagnetic-like cobalt clusters to which iron is bound tightly by a strong Fe-Co magnetic exchange interaction. The size of these clusters, and consequently their characteristic relaxation time as well as their characteristic magnetic field may have a temperature dependent distribution in the sample. A strong Fe-Co magnetic exchange interaction can result, even above $T \approx 150$ K, in the formation of locally ordered magnetic clusters consisting of iron as a nucleation centre along with a few neighboring Co cations being ordered because of their preferred magnetic orientation relative to that of the nucleation centre.

At the same time, in contrast to results published in [4], and in agreement with [13,14], $La_{0.8}Sr_{0.2}\,^{57}Fe_{0.05}Co_{0.95}O_{3-\delta}$ does not display considerable magnetoresistance above $T \approx 150$ K.

The ^{57}Fe Mössbauer parameters (Tabs. 1–2) clearly reflect that iron exists in the form of Fe^{3+} in the investigated systems. Thus, theories [16] that explain the effect of iron substitution on the electric properties of $La_{0.8}Sr_{0.2}Fe_xCo_{1-x}O_{3-\delta}$ by a preferred formation of Fe^{4+} instead of Co^{4+} cannot hold. Our results do not exclude, however, the possibility of occasional hopping of an electron from Fe^{3+} to a neighboring cobalt cation. But any Fe^{4+} cation formed in this way must have a very short lifetime compared to the mean lifetime of the ^{57}Fe nucleus, such that the probability of finding iron in the Fe^{4+} state is negligible compared to the probability that we find it in the Fe^{3+} state.

5 Conclusions

^{57}Fe Mössbauer spectroscopy and AC magnetic susceptibility measurements revealed that below $T \approx 65$ K $La_{0.8}Sr_{0.2}\,^{57}Fe_{0.05}Co_{0.95}O_{3-\delta}$ develops a cluster glass magnetic phase. The relaxation of iron magnetic moments, revealed by the ^{57}Fe Mössbauer spectra, was interpreted as an evidence for the existence of small superparamagnetic-like cobalt clusters. It was suggested that in $La_{0.8}Sr_{0.2}\,^{57}Fe_{0.05}Co_{0.95}O_{3-\delta}$ iron serves as a nucleation centre for magnetically ordered small Co clusters due to a strong Fe-Co magnetic exchange interaction.

Magnetotransport measurement has shown that in $La_{0.8}Sr_{0.2}\,^{57}Fe_{0.05}Co_{0.95}O_{3-\delta}$ above $T \approx 150$ K the magnetoresistance effect is negligible.

On the basis of the ^{57}Fe Mössbauer parameters of $La_{0.8}Sr_{0.2}\,^{57}Fe_{0.05}Co_{0.95}O_{3-\delta}$ the assumed [16] presence of a preferential electronic charge compensation $Fe^{3+} \rightarrow Fe^{4+}$ over that of $Co^{3+} \rightarrow Co^{4+}$ could be excluded in this compound.

Support by the Hungarian Science Foundation OTKA (F 034837, T 034839, T 037976, T043681, T043687 and T 043565) and the Hungarian Austrian Action Fund 56ou6 is gratefully appreciated. Z. Klencsár acknowledges the support from the Hungarian Bolyai János research grant.

References

1. J. Fontcuberta, Physics World, Feb. 1999
2. K.-I. Kobayashi, T. Kimura, H. Sawada, K. Terakura, Y. Tokura, Nature **395**, 677 (1998)
3. A.P. Ramirez, R.J. Cava, J. Krajewski, Nature **386**, 156 (1997)
4. A. Barman, M. Ghosh, S. Biswas, S.K. De, S. Chatterjee, Appl. Phys. Lett. **71**, 3150 (1997)
5. C. Zener, Phys. Rev. **82**, 403 (1951)
6. Q. Li, J. Zang, A.R. Bishop, C.M. Soukoulis, Phys. Rev. B **56**, 4541 (1997)
7. A.J. Millis, Nature **392**, 147 (1998)
8. V. Golovanov, L. Mihály, A.R. Moodenbaugh, Phys. Rev. B **53**, 8207 (1996)
9. R. Mahendiran, A.K. Raychaudhuri, Phys. Rev. B **54** (22), 16044 (1996)
10. S. Yamaguchi, H. Taniguchi, H. Takagi, T. Arima, Y. Tokura, J. Phys. Soc. Jpn **64**, 1885 (1995)
11. J. Wu, C. Leighton, Phys. Rev. B **67**, 174408 (2003)
12. A. Mineshige, M. Inaba, T. Yao, Z. Ogumi, J. Solid State Chem. **121**, 423 (1996)
13. A. Maignan, C. Martin, M. Hervieu, B. Raveau, Eur. Phys. J. B **13**, 41 (2000)
14. A.S. Ioselevich. Phys. Rev. Lett. **71**, 1067 (1993)
15. Á. Cziráki, I. Geröcs, M. Köteles, A. Gábris, L. Pogány, I. Bakonyi, Z. Klencsár, A. Vértes, S.K. De, A. Barman, M. Ghosh, S. Biswas, S. Chatterjee, B. Arnold, H.D. Bauer, K. Wetzig, C. Ulhaq-Bouillet, V. Pierron-Bohnes, Eur. Phys. J. B **21**, 521 (2001)
16. L.-W. Tai, M.M. Nasrallah, H.U. Anderson, D.M. Sparlin, S.R. Sehlin, Solid State Ionics **76**, 259 (1995)
17. Z. Klencsár, E. Kuzmann, A. Vértes, J. Radioanal. Nucl. Chem. **210**, 105 (1996)
18. R.H. Herber, *Chemical Mössbauer Spectroscopy* (Plenum Press, New York, 1984)
19. R. Caciuffo, J. Mira, J. Rivas, M.A. Senaris-Rodriguez, P.G. Radaelli, F. Carshugi, D. Fiorani, J.B. Goodenough, Europhys. Lett. **45**(3), 399 (1999)
20. R. Caciuffo, D. Rinaldi, G. Barucca, J. Mira, J. Rivas, M.A. Senaris-Rodriguez, P.G. Radaelli, D. Fiorani, J.B. Goodenough, Phys. Rev. B **59**(2), 1068 (1999)